J Therm Anal Calorim (2015) 120:1811–1817
DOI 10.1007/s10973-015-4498-z

Production and pyrolysis characteristics of citral–monochlorotriazinyl-β-cyclodextrin inclusion complex

Guangyong Zhu · Nienie Feng · Zuobing Xiao · Rujun Zhou · Yunwei Niu

Received: 5 September 2014 / Accepted: 26 January 2015 / Published online: 19 February 2015

Abstract Encapsulation aims at protecting components, providing controlled release, preventing oxidation and extending the shelf life. The inclusion complex of citral and monochlorotriazinyl-β-cyclodextrin has been studied. The scanning electron microscopy result showed that the dried citral–monochlorotriazinyl-β-cyclodextrin inclusion complexes formed aggregates with many geometric shapes in the size range 1–2 μm, and the transmission electron microscopy result shows that the inclusion complex aggregates were expressed through a bicontinuous "worm-type" pore system. Fourier transform infrared spectroscopy results show that citral enters the cavity of monochlorotriazinyl-β-cyclodextrin. The citral loading capacity determined from thermogravimetric data is about 8.96 %, and a 1:1 stoichiometry is obtained. Pyrolysis characteristics of the inclusion complexes were determined. Geometries of host, guest and the host–guest inclusion complex were optimized using molecular mechanics calculations. The binding energies for the most stable complexes geranial/monochlorotriazinyl-β-cyclodextrin and neral/monochlorotriazinyl-β-cyclodextrin are −143 and −162 kJ mol^{-1}, respectively. The shapes and orientations of those complexes were presented.

Keywords Pyrolsis characteristics · Citral–monochlorotriazinyl-β-cyclodextrin inclusion complex · Morphology · Binding energy · Molecular mechanics

G. Zhu · N. Feng · Z. Xiao (✉) · R. Zhou · Y. Niu
Shanghai Institute of Technology, Shanghai 201418, People's Republic of China
e-mail: zbingxiao@sina.com

Introduction

Flavor and fragrance play important roles and have been widely used in many products [1]. Citral is a common fragrance and flavor raw material. Citral has a strong, lemon-like odor and a characteristic bitter sweet taste. Commercially, the product is a mixture of two geometric isomers, i.e., geranial and neral (see Fig. 1). Geranial has a strong lemon odor. Neral's lemon odor is less intense, but sweeter. Citral is therefore an aroma compound used in perfumery for its citrus effect and is also used as a flavor and for fortifying lemon oil. Due to the inherent volatility of aroma ingredients in general, the lifespan of citral is short. The sensory perception can also be changed as a result of heating, oxidation, chemical interactions or volatilization. Indeed, perfume delivery systems that maintain the sensation of fragrance over extended periods of time are of interest. Among the many different alternatives available, the dynamic release by host–guest inclusion complexes is recognized as being highly promising. Cyclodextrins (CDs) are particularly well suited to host–guest inclusion complex interactions given their inherent cavity geometry [2–4]. CDs are very often used for protection and controlled release of food and pharmaceutical compounds. The molecular structure of CDs having a hydrophobic inner cavity allows to encapsulate geometrically compatible hydrophobic molecules. The hydrophilic exterior of CDs provides water solubility. As a result of this guest–host interaction, the hydrophobic compounds can be "transformed" in solid products with better aqueous solubility, having higher stability against oxygen/air, light, or other degradative factors and controlled release properties [5].

As a derivative of β-CD, monochlorotriazinyl-β-cyclodextrin (MCT-β-CD) has been widely used in fabric finishing including antibacterial, antistatic, anti-insect, surface

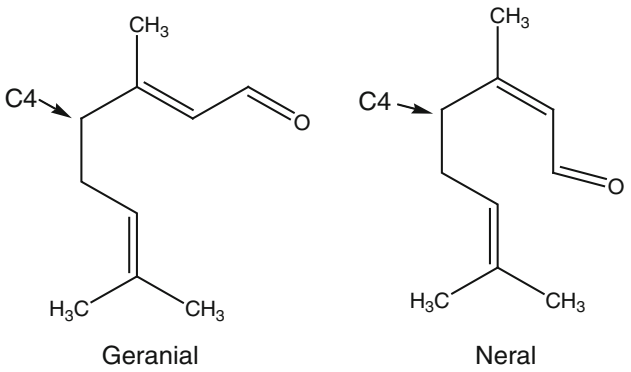

Fig. 1 Molecular formulas of geranial and neral

modification, UV protecting and other applications [6, 7]. MCT-β-CD possesses monochlorotriazinyl groups as reactive anchor and can form stable covalent bonds with nucleophilic groups, such as –OH in cellulose. Therefore, MCT-β-CD offers the possibility to encapsulate some aromatic compounds and to immobilize them on a cellulose surface such as paper, cotton and other textile materials, providing an interesting way in surface modification and maintaining the sensation of aroma over extended periods of time.

In the present work, the inclusion complexes of MCT-β-CD with citral were produced and characterized by transmission electron microscopy (TEM), scanning electron microscopy (SEM), Fourier transform infrared (FTIR) spectroscopy, thermogravimetric (TG) analysis. Molecular mechanics (MM) is a nonquantum mechanical method of computing structures, energies and some properties of molecules [8]. The binding of citral to MCT-β-CD was investigated by MM2.

Experimental

Materials

Citral (food grade) was obtained from the Peking University Zoteq Co., Ltd. Monochlorotriazinyl-β-cyclodextrin (with content 75 % and average molecular weight 1,560) was purchased from Yongtai Biotech Co., Ltd (Xi'an, China). Anhydrous ethanol and sodium carbonate (analytical grade) were purchased from Sinopharm Chemical Reagent Co., Ltd (Shanghai, China). All reagents were used without further purification. Deionized water was used throughout the experiments.

Preparation of the MCT-β-CD inclusion complex

Preparation of the inclusion complex was carried out as follows: 5 g MCT-β-CD was added in 70 mL deionized water. A 524G digital electromotive stirrer (Shanghai, China) was used to dissolve it. Then citral was added dropwise to the aqueous solution of MCT-β-CD and stirred at 1,000 rpm for 10 h to form citral–MCT-β-CD inclusion complex. Drying was carried out in a FD-1C-50 freeze-drier (Beijing, China) for 48 h at a temperature lower than −50 °C and pressure of around 20×10^{-3} kPa. The dried samples were collected and stored in a desiccator at room temperature prior to further TG and FTIR analysis.

TEM measurement

TEM measurement was taken using a FEI Tecnai electron microscopy at an acceleration voltage of 200 kV to investigate the morphology of citral–MCT-β-CD inclusion complex. The citral–MCT-β-CD inclusion complex aqueous solution was dripped onto a 300-mesh copper grid-coated carbon film. The sample was dried before viewing on the TEM.

SEM measurement

SEM (S-3400N, Hitachi High-Technologies, Tokyo, Japan) was used to observe the appearance of citral–MCT-β-CD inclusion complex. The citral–MCT-β-CD inclusion complex samples were coated with a thin layer of sputtered gold prior to examination. The SEM image of the citral–MCT-β-CD inclusion complexes was conducted at an accelerating voltage of 15 kV.

Thermogravimetric (TG) analysis

The experiments were carried out in a TGA-Q5000IR TG analyzer (TA Instruments, USA). In the experiment, approximately 5 mg of dried sample was spread uniformly on the bottom of the ceramic crucible of the thermal analyzer. The pyrolysis experiment was performed at a heating rate of 5 °C min^{-1} in a dynamic high purity nitrogen flow of 20 mL min^{-1}. The temperature of the furnace was programmed to rise from room temperature to 600 °C.

Fourier transform infrared (FTIR) spectroscopy

FTIR spectra of citral, blank sample and freeze-dried inclusion complex were characterized by IR spectrometry (IRAffinity-1, Shimadzu Company, Japan) in the frequency range of 4,000–400 cm^{-1} with resolution of 2 cm^{-1}.

Molecular mechanics calculations

Molecular mechanics uses an empirical force field, which is a mathematical recipe for reproducing a molecule's potential energy surface (the location and motion of nuclei

on such surfaces dictate a molecule's structure and dynamical properties) [8]. The formation of citral–MCT-β-CD inclusion complex at the molecular level is examined using MM2 calculations, which can provide some information regarding the energy and structure of inclusion complexes. All calculations were performed with Chem3D Ultra (CambridgeSoft Corporation, MA, USA). Geometries of host, guest and the host–guest inclusion complex were optimized using MM2 calculations.

Due to the fact that MCT-β-CD is relatively large, flexible molecule that is studied experimentally in aqueous environments, this makes computations on them prohibitive or, as often is the case, forces one to introduce so many assumptions and impose so many restrictions so as to become unrealistic. MM2 might allow for the correct determination of the complex geometry and correctly reproduce experimental data without consideration of solvent effects in the host–guest complexation process according to literatures [9–11]. Although there was limitation (absence of solvent) in the method, solvent was not considered neither implicitly nor explicitly during calculation. After properly orienting host and guest, the inclusion process was simulated by successively changing the *Z* coordinate of the guest atoms. The position of the guest relative to the host is referred to the *Z* coordinate of one reference atom (C4 as shown in Fig. 1) of the guest. There are several isomers of substituted MCT-β-CD. 1,3,5-trisubstituted MCT-β-CD has the lowest energy and can be considered as main component of MCT-β-CD [6]. Therefore, 1,3,5-trisubstituted MCT-β-CD is used to study the binding energy (BE) of citral–MCT-β-CD inclusion complex. The guest moving direction during the complexation processes was shown in Fig. 2. The labeled carbon atom (C4) of the guest molecule is used to express the relative position between the guest and host when the guest passes through the cavity of the MCT-β-CD.

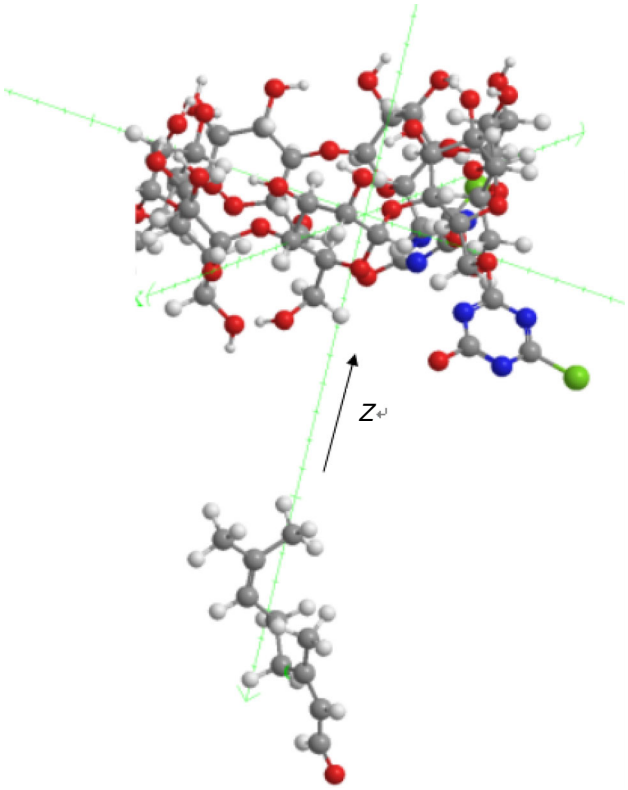

Fig. 2 Moving direction of the guest during the complexation processes

Results and discussions

The appearance and shape of citral–MCT-β-CD inclusion complex

The relatively hydrophobic cavity of MCT-β-CD can accommodate citral to form inclusion complex. The inclusion complex of citral with MCT-β-CD was observed by SEM and TEM. The SEM image of the citral–MCT-β-CD inclusion complex is shown in Fig. 3. As shown in Fig. 3, citral–MCT-β-CD inclusion complexes are able to form aggregates during the drying process. The aggregates have many geometric shapes. The distribution of the particle sizes of the dried citral–MCT-β-CD inclusion complexes is mostly in the size range 1–2 μm.

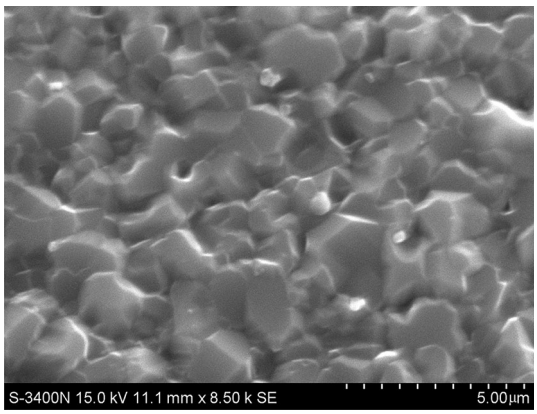

Fig. 3 SEM image of the citral–MCT-β-CD inclusion complexes

The TEM image of the citral–MCT-β-CD inclusion complex is shown in Fig. 4. As shown in Fig. 4, wormlike structure can be found. Like other CDs, it suggested that the citral–MCT-β-CD inclusion complex aggregates were expressed through a bicontinuous "worm-type" pore system. This wormlike structure like β-CD was also reported in the literatures [12, 13]. In addition, the obvious lattice fringe can be found in the TEM image. It may be assigned to crystalline planes of NaCl, the main impurity in MCT-β-CD. During the synthesis process of MCT-β-CD, NaCl is a

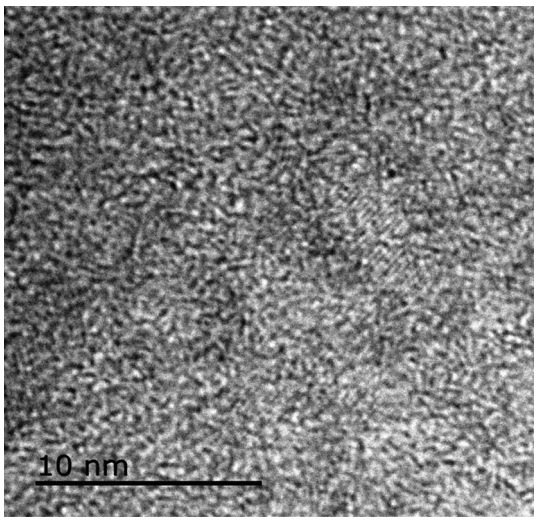

Fig. 4 TEM image of the citral–MCT-β-CD inclusion complexes

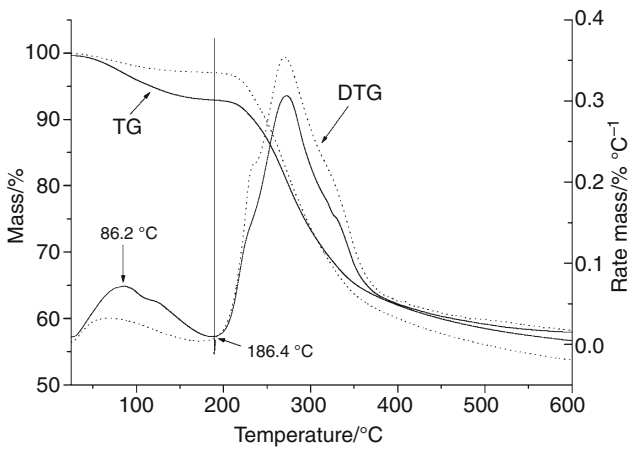

Fig. 5 TG–DTG curves of blank MCT-β-CD (*broken line*) and citral–MCT-β-CD inclusion complex (*real line*)

by-product. MCT-β-CD was used without further purification in the experiments.

Pyrolysis characteristics of citral–MCT-β-CD inclusion complex

In order to investigate the combination of citral and MCT-β-CD, TG was employed in the experiment. TG is a method of thermal analysis in which changes in physical and chemical properties of materials are measured as a function of increasing temperature, or as a function of time [1, 14]. Figure 5 shows the mass loss and the rate of mass loss curve obtained during the pyrolysis of blank MCT-β-CD and citral–MCT-β-CD inclusion complex samples under inert atmosphere at a heating rate of 5 °C min^{-1}. As shown in Fig. 5, during thermal degradation, three main stages can be distinguished from the TG curves of both blank MCT-β-CD and citral inclusion complex samples. The first stage goes from room temperature to 186.4 °C; a slight mass loss in the TG curve is observed. The second stage goes from 186.4 to 385.1 °C and is characterized by a major mass loss, which corresponded to the main pyrolysis process of MCT-β-CD. Most of MCT-β-CD was decomposed in this stage. Two strong peaks appeared at 272.8 °C in the DTG curves of both blank and encapsulated samples and were due to the decomposition of MCT-β-CD. At this temperature, the rate of mass loss attained the maximum value. The third stage goes from 385.1 °C to the final temperature (600 °C) of the experiment. The solid residuals continuously decomposed at a very slow rate in the third stage. The content of MCT-β-CD is 75 %. There are about 25 % NaCl in the MCT-β-CD sample. Therefore, the content of the solid residuals is high as shown in Fig. 5.

Compared to the pyrolysis characteristic of blank MCT-β-CD, the TG curve of blank MCT-β-CD shows a leveling off from room temperature to 186.4 °C, while the TG curve of citral–MCT-β-CD inclusion complex is downward sloping in this temperature range. Furthermore, two peaks can be observed in the derivative thermogravimetric (DTG) curves in the first stage. The peak of citral–MCT-β-CD inclusion complex is larger than that of blank MCT-β-CD. The small peak of blank MCT-β-CD is mainly attributed to vaporization of water. Upon complexation of rather hydrophobic guest, all the water molecules might be expelled from the internal cavity to the CD periphery during the inclusion process [9–11]. Therefore, the peak of citral–MCT-β-CD inclusion complex at 86.2 °C on the first stage is mainly attributed to vaporization of citral encapsulated in MCT-β-CD. The mass losses of blank of MCT-β-CD and citral–MCT-β-CD inclusion complex from room temperature to 186.4 °C are 3.8 and 8.96 %, respectively. From the value of mass loss of citral–MCT-β-CD inclusion complex, citral loading capacity can be estimated. Because of the hydrophobic character of citral molecule under investigation, the water that is included in MCT-β-CD complexes can be ignored. Therefore, the citral loading capacity is about 8.96 %. During the thermal degradation of citral–MCT-β-CD inclusion complex, the encapsulated citral was gradually released. Citral release mainly happened in the first stage of the TG curve as shown in Fig. 5. The average molecular weight of MCT-β-CD is 1,560, and the molecular weight of citral is 152. If 1:1 host:guest stoichiometry is considered, the theoretical citral loading capacity is 8.88 %. This value corresponds closely to the pyrolysis result, 8.96 %. So the ratio of MCT-β-CD to citral for the inclusion complex is approximately 1:1.

FTIR results of citral, MCT-β-CD and its inclusion complexes

The FTIR spectra of citral, MCT-β-CD and its inclusion complexes are presented in Fig. 6, and the main IR absorbance bands are marked. As shown in Fig. 2 (curve a), there is a band locating at 1,649 cm^{-1} which can be assigned to the stretching (C=O) vibration of the carbonyl group. The stretching (O–H) vibration of the hydroxyl on β-CD appears at 3,428 cm^{-1}. The stretching (C–H) vibration of methane occurs at 2,932 cm^{-1}, and its wagging (C–H) vibration appears at 1,410, 1,359, 1,288 cm^{-1}. The scissoring (CH_2) vibration of methylene can be observed at 1,467 cm^{-1}. The stretching (C–O) vibration appears at 1,155, 1,082 and 1,028 cm^{-1}. The main vibration bands of monochloroazinyl group can also be observed in FTIR spectrum. The (C=N) vibration of triazine ring appears at 1,568 cm^{-1}. The breath vibration of triazine ring appears at 916 cm^{-1} and its in-plane and out-of-plane deformation vibration appears at 820 cm^{-1} [6].

As shown in Fig. 6 (curve b), the IR spectrum of the inclusion complex is similar to that of MCT-β-CD (curve a), indicating that the frame of MCT-β-CD in the complex is not changed. Encapsulation of citral does not significantly change the spectrum of MCT-β-CD.

Citral had a very strong absorption band at 1,674 cm^{-1} for the C=O stretching vibration as shown in Fig. 6 (curve c). The peaks at 2,916 and 2,847 cm^{-1} can be assigned to stretching (CH_3 and CH_2) vibration. The (C=C) vibration appears at 1,443 cm^{-1}. The bending (CH3) vibration appears at 1,380 cm^{-1} [15]. In the IR spectrum of the inclusion complex, the peaks of citral at 2,966, 2,916, 2,860, 2,759 and 1,674 cm^{-1} were disappeared or shifted to other wave numbers. These changes could be attributed to the fact that citral enters the cavity of MCT-β-CD.

MM2 calculations

In general, BE represents the mechanical work which must be done against the forces which hold an object together [1]. Therefore, the investigation of the BE of citral and MCT-β-CD is important for a deep understanding of the interaction between citral and MCT-β-CD, and the reaction mechanism. It can help us reveal the combination of the host and the guest. The BE can be expressed as

$$\mathrm{BE} = E_{\mathrm{complex}} - E_{\mathrm{guest}} - E_{\mathrm{host}} \quad (1)$$

where E_{complex} is the total energy of the inclusion complex, E_{guest} is the sum of total energy of guests, and E_{host} is the total energy of host. The more negative the BE is, the more thermodynamically favorable is the inclusion complex [16].

The initial docking strategy was to push the citral stepwise through the cyclodextrin orifice minimizing the energy of the complex at each step. The guest position throughout the study is referred to by the *Z* coordinate of its C4 atom. The energy variation associated with the inclusion process was computed for citral as shown in Fig. 7. The solid and dashed lines are for the neral and geranial inclusions, respectively. The binding energies for the most stable complexes geranial/MCT-β-CD and neral/MCT-β-CD are −143 and −162 kJ mol^{-1} at -1.8×10^{-10} and 3.8×10^{-10} m, respectively.

The MM2-computed structures for both energy minima are shown in Fig. 8. Once the guest is included, MCT-β-CD can change its shape (induced fit binding) and it does

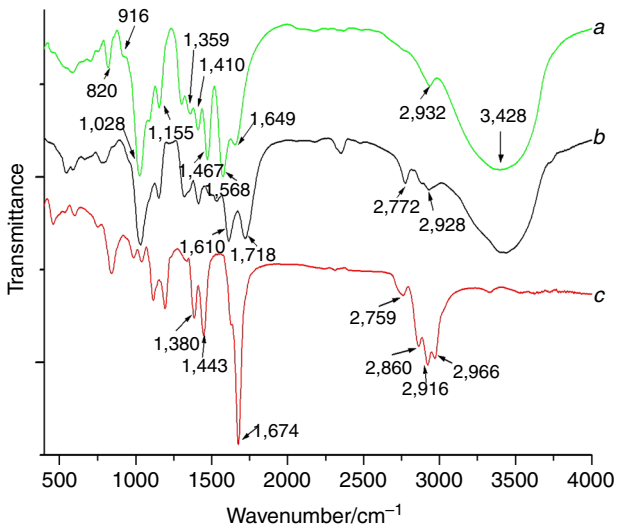

Fig. 6 FTIR spectra of MCT-β-CD (*a*), citral/MCT-β-CD inclusion complex (*b*), citral (*c*)

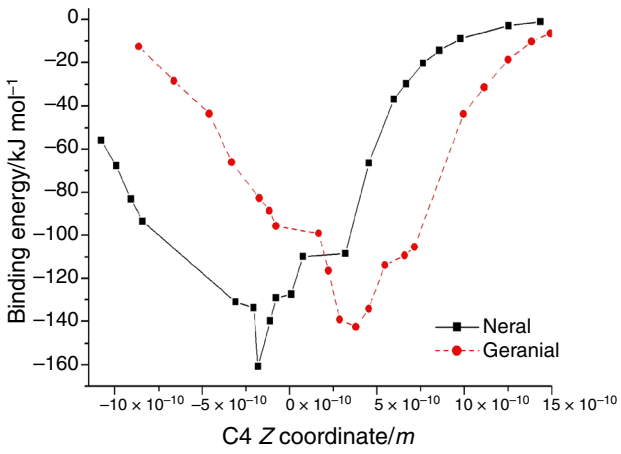

Fig. 7 Plotting of calculated binding energy versus the *Z* coordinate of the C4 in the guest molecule

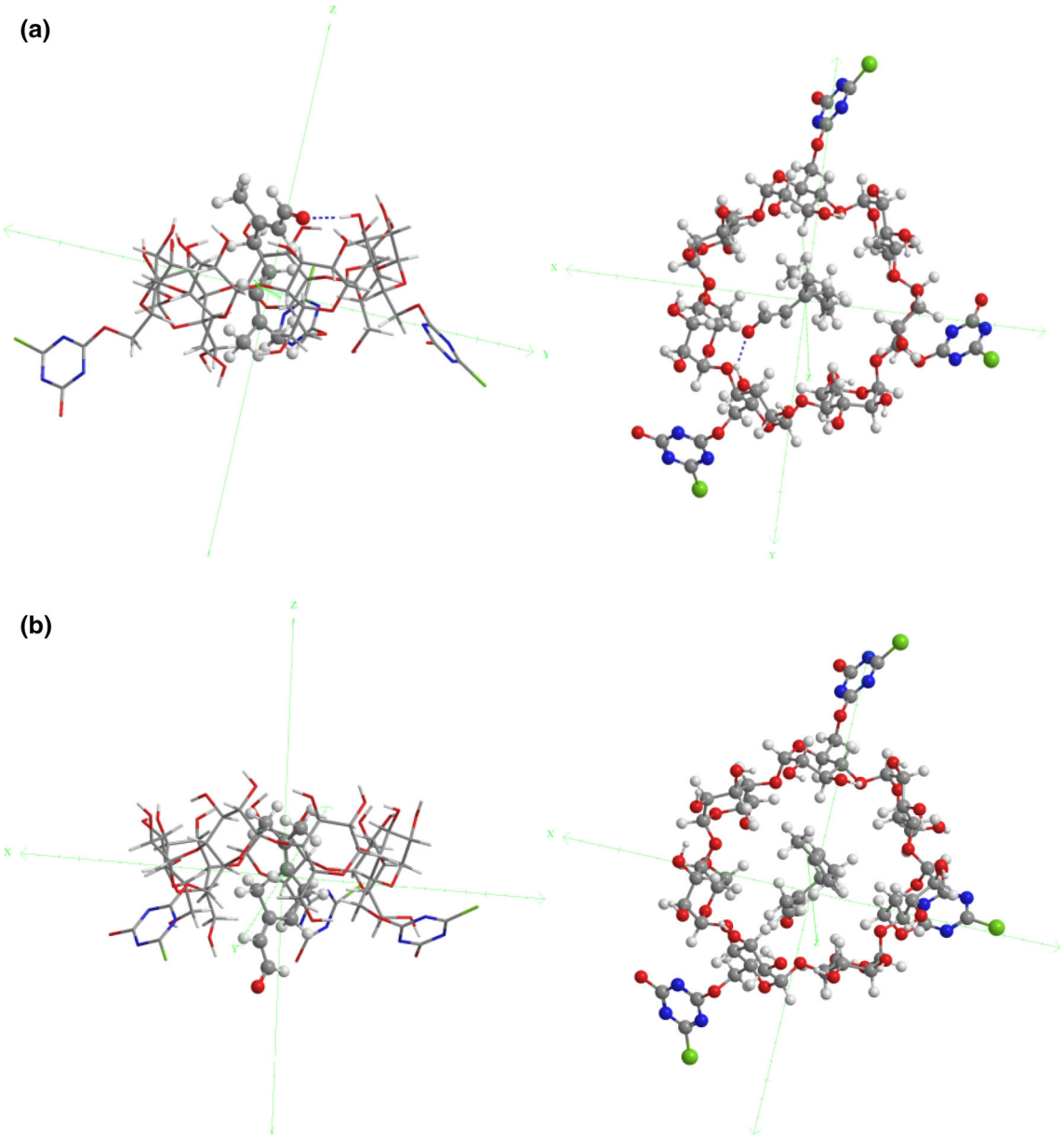

Fig. 8 Structures of the energy minima obtained by the MM2 calculations for the MCT-β-CD/citral inclusion complex (**a** geranial, **b** neral)

so to maximize the stabilization. The guest molecule also made conformational adjustments to take maximum advantage of the weak van der Waals forces that exist, and the complexation geometry of the guest was constantly re-adjusted until the most stable supramolecular interactions were gained during the MM2 calculations, and finally, the energy changes were recorded. The binding of guest molecules within the host MCT-β-CD is not fixed or permanent but rather is a dynamic equilibrium. Binding strength depends on how well the 'host–guest' complex fits together and on specific local interactions between surface atoms, such as van der Waals forces, hydrophobic interactions and hydrogen bonds [16, 17].

Conclusions

This paper deals with the production and characterization of citral–MCT-β-CD inclusion complex. The inclusion complexes were produced and characterized by TEM, SEM, FTIR and TG. The result of the morphology of the inclusion complexes showed that the dried citral–MCT-β-CD inclusion complexes formed aggregates with many geometric shapes in the size range 1–2 μm. These aggregates were expressed through a bicontinuous "worm-type" pore system. FTIR results confirm that citral enters the cavity of MCT-β-CD. The citral loading capacity is about 8.96 %. A 1:1 host:guest stoichiometry is obtained.

Geometries of host, guest and the host–guest inclusion complex were optimized using MM2 calculations. The binding energies of the inclusion complexes were obtained, and the shapes and orientations of those complexes were presented. The binding energies for the most stable complexes geranial/MCT-β-CD and neral/MCT-β-CD are -143 and -162 kJ mol^{-1} at -1.8×10^{-10} and 3.8×10^{-10} m, respectively.

Acknowledgements This work was financially supported by the National Natural Science Fund of China (21276157, 21476140).

References

1. Zhu G, Xiao Z, Zhou R, Zhu Y. Study of production and pyrolysis characteristics of sweet orange flavor-β-cyclodextrin inclusion complex. Carbohydr Polym. 2014;105:75–80.
2. Schofield WCE, Badyal JPS. Controlled fragrant molecule release from surface-tethered cyclodextrin host-guest inclusion complexes. Appl Mater Interfaces. 2011;3:2051–6.
3. Menezes PP, Serafini MR, Quintans-Júnior LJ, Silva GF, Oliveira JF, Carvalho FMS, Souza JCC, Matos JR, Alves PB, Matos IL, Hădărugă DI, Araújo AAS. Inclusion complex of (–)-linalool and β-cyclodextrin. J Therm Anal Calorim. 2014;115:2429–37.
4. Serafini MR, Menezes PP, Costa LP, Lima CM, Quintans LJ Jr, Cardoso JC, Matos JR, Soares-Sobrinho JL, Grangeiro S Jr, Nunes PS, Bonjadim LR, Araújo AAS. Interaction of *p*-cymene with β-cyclodextrin. J Therm Anal Calorim. 2012;109:951–5.
5. Heghes A, Hădărugă NG, Fulias A-V, Bandur GN, Hădărugă DI, Dehelean C-A. *Capsicum annuum* extracts/β-cyclodextrin complexes. J Therm Anal Calorim. 2014;. doi:10.1007/s10973-014-4229-x.
6. Yao Q, You B, Zhou S, Chen M, Wang Y, Li W. Inclusion complexes of cypermethrin and permethrin with monochlorotriazinyl-beta-cyclodextrin: a combined spectroscopy, TG/DSC and DFT study. Spectrochim Acta A. 2014;117:576–86.
7. Vrinceanu N, Tanasa D, Hristodor CM, Brinza F, Popovici E, Gherca D, Pui A, Coman D, Carsmariu A, Bistricianu I, Broasca G. Synthesis and characterization of zinc oxide nanoparticles. J Therm Anal Calorim. 2013;111:1107–19.
8. Lipkowitz KB. Applications of computational chemistry to the study of cyclodextrins. Chem Rev. 1998;98:1829–73.
9. Salvatierra S, Jaime C, Virgili A, Sánchez-Ferrando F. Determination of the inclusion geometry for the γ-cyclodextrin/benzoic acid complex by NMR and molecular modeling. J Org Chem. 1996;61:9578–81.
10. Fathallah M, Fotiadu F, Jaime C. Cyclodextrin inclusion complexes. MM2 calculations reproducing bimodal inclusions. J Org Chem. 1994;59:1288–93.
11. Pérez F, Jaime C, Sánchez-Ruiz X. MM2 calculations on cyclodextrins: multimodal inclusion complexes. J Org Chem. 1995;60:3840–5.
12. Polarz S, Smarsly B, Bronstein L, Antonietti M. From cyclodextrin assemblies to porous materials by silica templating. Angew Chem Int Ed. 2001;40:4417–21.
13. He Y, Fu P, Shen X, Gao H. Cyclodextrin-based aggregates and characterization by microscopy. Micron. 2008;39:495–516.
14. Zhu G, Xiao Z, Zhou R, Feng N. Production of a transparent lavender flavour nanocapsule aqueous solution and pyrolysis characteristics of flavour nanocapsule. J Food Sci Technol. 2014;. doi:10.1007/s13197-014-1465-9.
15. Zhou W, Lin J, Wu R, Lin W, Ge F, Huang H. Direct synthesis of lemonile from litsea cubeba oil. Fine Chem. 2005;22:515–7 (in Chinese).
16. Zeng Z, Fang Y, Ji H. Side chain influencing the interaction between b-cyclodextrin and vanillin. Flavour Fragr J. 2012;27:378–85.
17. Yang Z, Zeng Z, Xiao Z, Ji H. Preparation and controllable release of chitosan/vanillin microcapsules and their application to cotton fabric. Flavour Fragr J. 2014;29:114–20.